

# A Novel Channel Reconstruction Method for Multi-User Over-the-Air Testing

Mengjie Yan, Zhengbo Jiang, *Member, IEEE*, Wei Fan, *Member, IEEE*, Chong Guo, Fan Wu, *Member, IEEE*,

Kin-Fai Tong, *Fellow, IEEE*, and Wei Hong, *Fellow, IEEE*

**Abstract**—Most existing research on over-the-air (OTA) testing has focused on single-user scenarios but is ineffective for evaluating system performance of multi-users, due to the difficulty of precisely constructing multiple channels in a microwave anechoic chamber. This paper presents a system model for multi-user OTA testing and employs the Whale Optimization Algorithm (WOA) to compute the pre-compensation matrix, which aims to eliminate the interference between multiple users. Experimental results demonstrate that the proposed scheme can construct different channels for two users in a microwave anechoic chamber, with an inter-user isolation greater than 15 dB, illustrating the feasibility of multi-user OTA testing.

**Index Terms**—Channel reconstruction, multi-user, over-the-air (OTA) testing, wireless cable.

## I. INTRODUCTION

MASSIVE MIMO is a one of the key technologies in the fifth or sixth generation of mobile communication (5G/6G) [1]. The base station (BS) is equipped with hundreds or even thousands of antennas, serving multiple user equipment (UEs) with various wireless channel environments. In a multi-user MIMO system, specific algorithm is always employed to enhance the system performance for the corresponding channel [2]. Consequently, compared to single-user scenarios, system performance for multi-user can vary significantly. Over-the-air (OTA) testing is an essential way to evaluate the system performance of 5G/6G equipment.

At present, most of the research of OTA system performance testing focuses on single-user scenarios, with limited studies addressing multi-user cases [3]. Most commercial testing solutions for multi-user scenarios have been done in the conducted setup. Note that OTA testing for multi-user is not a simple extension for the single-user OTA testing. As shown in Fig. 1, the key challenge is that the spatial profiles for each user, which might be highly different or similar depending on the spatial locations of the users, should be accurately reconstructed over-the-air, without any cross-talks [4].

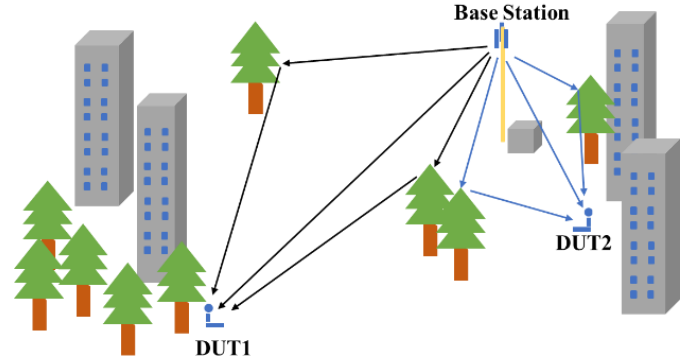


Fig. 1. Multi-user communication scenario.

Reconstructing the wireless channel environment in an anechoic chamber is one of the most critical aspects of OTA system performance testing. The key issue to be solved in multi-user OTA testing is to construct multiple channel environments within a specified spatial area. Several OTA methods have been investigated in the literature to address the challenges of radio performance testing [5][6][7]. The Reverberation Chamber (RC) uses a metal stirrer to stir electromagnetic waves in a shielded cavity, thereby producing a multipath environment similar to random distribution, simulating rich multipath Rayleigh fading channels [8]. However, it is evidently unable to generate multiple distinct channels within the same shielded cavity. On the other hand, the Multi-Probe Anechoic Chamber (MPAC) places multiple antenna probes at different positions within the anechoic chamber to simulate multiple angles of arrival or departure, thereby constructing a spatial channel environment [9]. Theoretically, MPAC has a stronger spatial construction capability, but most research efforts so far have focused on single-user channel construction.

The primary challenge in constructing multi-user channels within an anechoic chamber is how to eliminate the inter-user interference, which is one of the main errors in reconstructing multi-user channels. In recent years, wireless cable methods have been proposed to replace the traditional conductive connection, i.e. one-to-one transmission between two transmitting antennas and two receiving antennas, by reducing

This work was supported by the National Key Research and Development Program of China under Grant 2020YFB1804900. (*Corresponding authors: Zhengbo Jiang*)

Mengjie Yan, Zhengbo Jiang, Wei Fan, Fan Wu and Wei Hong are with School of Information Science and Engineering, Southeast University, Nanjing 211189, China (email: mengjieyan@seu.edu.cn; jzb@seu.edu.cn; weifan@seu.edu.cn; fan.wu@seu.edu.cn; weihong@seu.edu.cn).

Chong Guo is with Meatron Electronics, Nanjing 210096, China (e-mail: chongguo@meatronee.com).

K. -F. Tong is with the department of Electronic and Electrical Engineering, University College London, London, United Kingdom (e-mail: k.tong@ucl.ac.uk).

> REPLACE THIS LINE WITH YOUR MANUSCRIPT ID NUMBER (DOUBLE-CLICK HERE TO EDIT) <

interference from adjacent antennas [10]. The basic principle involves measuring the transmission matrix between the transmitting antenna array and the receiving antenna array, and then multiplying by its inverse transmission matrix at the transmitter end to obtain a diagonal matrix, thus achieving one-to-one virtual cable connections. The wireless cable method has been applied in single-user MIMO OTA testing[11].

To the best of the authors' knowledge, for the first time, this paper proposes a system model for multi-user OTA testing, with an optimization algorithm to reduce inter-user interference, and experimental validation is carried out to proof the effectiveness of the proposed method. The structure of this paper is arranged as follows. Section II presents the system model for multi-user OTA testing; Section III provides the Whale Optimization Algorithm (WOA) for computing the pre-compensation matrix; Section IV presents the measurement results and experimental validation; finally, Section V summarizes the paper.

## II. SYSTEM MODEL AND PROBLEM STATEMENT

### A. Traditional cabled setup

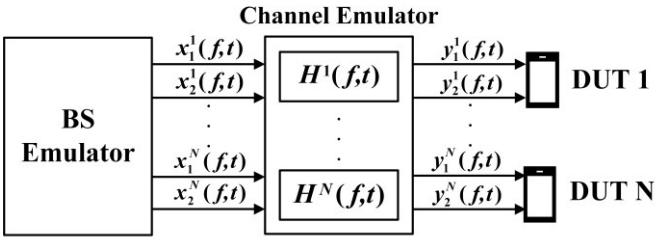


Fig. 2. The conductive testing for multi-user MIMO System.

The multi-user MIMO conduction testing system is shown in Fig. 2, which includes BS emulator, channel emulator (CE), and N DUTs. For simplicity of discussion, each DUT is assumed to be a two-element antenna array. The relationship between the input and output of the MIMO system for the  $n$ th DUT, ignoring noise terms, can be represented as

$$Y^n(f, t) = H^n(f, t)X^n(f, t), \quad (1)$$

where  $H^n(f, t) = \{h_{ij}^n(f, t)\}_{2 \times 2}$ , with  $h_{ij}^n(f, t)$  represents the time-varying channel frequency response (CFR) from the  $j$ th Tx antenna to the  $i$ th Rx antenna of the  $n$ th DUT at the CE port.  $Y^n(f, t) \in \mathbb{C}^{2 \times 1}$  is the received signal vector of the  $n$ th DUT;  $X^n(f, t) \in \mathbb{C}^{2 \times 1}$  is the transmit signal vector of the BS emulator corresponding to the  $n$ th DUT. In conducted testing, the specified test signal is transmitted directly to the corresponding DUT antenna port through the RF cable, and no crosstalk occurs between users. The antenna patterns on the Tx side and the Rx side can be embedded in the CFR implemented in the CE.

### B. Over-the-air setup

The following is a system for multi-user MIMO OTA testing using two DUTs as an example, as shown in Fig. 3. The BS has four Tx antennas and each DUT has two Rx antennas. The Tx

antenna sends signals to the DUT simultaneously. The relationship between the input and output of the multi-user MIMO OTA system is

$$\begin{aligned} \begin{bmatrix} Y^1 \\ Y^2 \end{bmatrix} &= \begin{bmatrix} A^1 \\ A^2 \end{bmatrix} [G^1 \ G^2] \begin{bmatrix} H^1 & 0 \\ 0 & H^2 \end{bmatrix} \begin{bmatrix} X^1 \\ X^2 \end{bmatrix} \\ &= \begin{bmatrix} A^1 G^1 H^1 X^1 + A^1 G^2 H^2 X^2 \\ A^2 G^1 H^1 X^1 + A^2 G^2 H^2 X^2 \end{bmatrix}, \end{aligned} \quad (2)$$

where transmission matrix is denoted as  $[A^1, A^2]$ , where  $A^n = \{a_{ij}^n\} \in \mathbb{C}^{2 \times 4}$  ( $n = 1, 2$ ) represent the transmission matrices from all Tx antennas of the CE to the first and second DUTs, respectively,  $a_{ij}^n$  is the unknown coupling coefficient of the  $i$ th Rx antenna of the  $n$ th DUT receiving the  $j$ th Tx antenna corresponding to the CE port.  $G^n = \{g_{ij}^n\} \in \mathbb{C}^{4 \times 2}$  is corresponding pre-compensation matrix to achieve  $A^n G^n = I_{2 \times 2}$ , with  $I_{2 \times 2}$  donating a  $2 \times 2$  identity matrix. For the  $n$ th DUT,  $Y^n$  can be expressed as

$$Y^n = A^n G^n H^n X^n + A^n \sum_{k=1, k \neq n}^2 G^k H^k X^k \quad (3)$$

It can be seen that the first term  $A^n G^n H^n X^n$  in the Eq. (3) represents the actual desired signal received by the  $n$ th DUT, and the second term  $A^n \sum_{k=1, k \neq n}^2 G^k H^k X^k$  is the interference signal for the  $n$ th DUT, i.e., multi-user interference. This term is the primary factor affecting the performance of multi-user MIMO systems OTA testing.

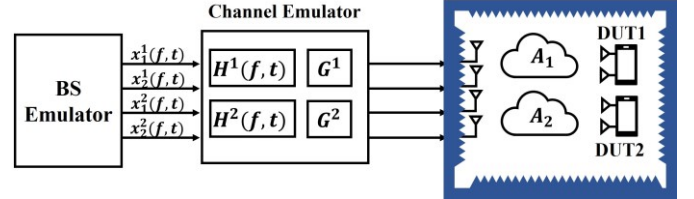


Fig. 3. Multi-user MIMO OTA testing system.

## III. METHOD

### A. Objective Function

As seen from Eq. (4), each DUT needs to achieve a wireless connection, which requires satisfying  $A^n G^n = I_{2 \times 2}$ . Additionally, it is necessary to mitigate interference from other DUTs, which means that each element of the matrix  $A^k G^n$  ( $k \neq n, k = 1, 2$ ) should be as small as possible. Therefore, an objective function can be constructed as

$$L(G^n, \lambda) = a \|A^n G^n\|_F + b (\|A^k G^n - I_{2 \times 2}\|_F), \quad (4)$$

where  $a$  and  $b$  are weight coefficients used to balance the weights of the two objectives;  $\|\cdot\|_F$  is the Frobenius norm,  $\|\cdot\|_F \stackrel{\text{def}}{=} \sqrt{\sum_i \sum_j x_{i,j}^2}$ . As shown in Eq. (3), if transmission matrix  $[A^1, A^2]$  is known, it can be calibrated out by implementing the pre-compensation matrix  $G^n$  in the CE.

### B. WOA Algorithms

As mentioned in the calibration procedure, we need to determine the pre-compensation matrix  $G^n$  to enable the  $n$ th

> REPLACE THIS LINE WITH YOUR MANUSCRIPT ID NUMBER (DOUBLE-CLICK HERE TO EDIT) <

DUT to achieve wireless connection without interference from other DUTs. Solving the pre-compensation matrix is essentially a mathematical inverse problem, and many algorithms can handle such issues such as Particle Swarm Optimization (PSO), Genetic Algorithm (GA), etc. In this paper, WOA algorithm is applied to determine  $G^n$ . WOA simulates the hunting behavior of whales, utilizing strategies such as encircling prey, spiral-shaped hunting, and random search[12].

The pseudo-code of the WOA algorithm is as follows:

---

**Algorithm 1** Whale Optimization Algorithm for Matrix  $G^n$  Optimization

---

```

1: Initialize matrices  $A1, A2$ 
2: Initialize target matrices  $M1, M2$ 
3: Define objective function as

   objective_function =  $0.7 \times \|10 \times \log_{10}(\|A1 \times B\|) - M1\|_F$ 
   +  $0.3 \times \|10 \times \log_{10}(\|A2 \times B\|) - M2\|_F$ 

4: Set whale optimization parameters:  $N\_whales = 50$ ,  $N\_iter = 500$ ,  $b = 1$ ,
    $l \in [-1, 1]$ ,  $a = 2 - t^*(2)/N\_iter$ ,
5: Initialize  $B\_population$ 
6:  $t \leftarrow 0$ 
7: while  $t < N\_iter$  do
8:   for each whale do
9:     Update parameters  $a, A, C, l, p$ 
10:    if  $p < 0.5$  then
11:      if  $|A| < 1$  then
12:        Update position using a random whale
13:      else
14:        Update position using the best whale
15:      end if
16:    else
17:      Update position using the spiral equation
18:    end if
19:    Map position to complex form with  $\alpha$  and  $\phi$ 
20:  end for
21: Check and correct whales out of bounds
22: Calculate fitness of each whale using the objective function
23: Update  $bestG$  if a better solution is found
24:  $t \leftarrow t + 1$ 
25: end while
26: return  $bestG$  and minimal objective value  $bestFval$ 

```

---

In this algorithmic framework, the population consists of several whales, each of which contains 8 complex variables. For each complex variable, the phase term  $\phi$  and amplitude term  $\alpha$  are constrained within the range of  $[-\pi, \pi]$  and  $[\alpha_{min}, \alpha_{max}]$ , respectively. The objective function for each DUT is given by Eq. (4). The population size  $N_{whales}$  is set to 50, representing the number of whales. The maximum number of iterations  $N_{iter}$  is set to 500, defining the maximum number of algorithm iteration. The coefficient vector  $a$  is initially 2 and decreases linearly to 0 to dynamically adjust the position of the whales. The spiral constant  $b$  is set to 1, which determines the shape of the spiral hunting. The initial random number  $l$  ranges from  $[-1, 1]$  and is used to calculate the spiral path. The criteria used in this paper is the maximum number of iterations  $N_{iter}$  or the required isolation threshold. Therefore, for each DUT, the complexity of WOA is limited by  $N_{whales} \times N_{iter}$ .

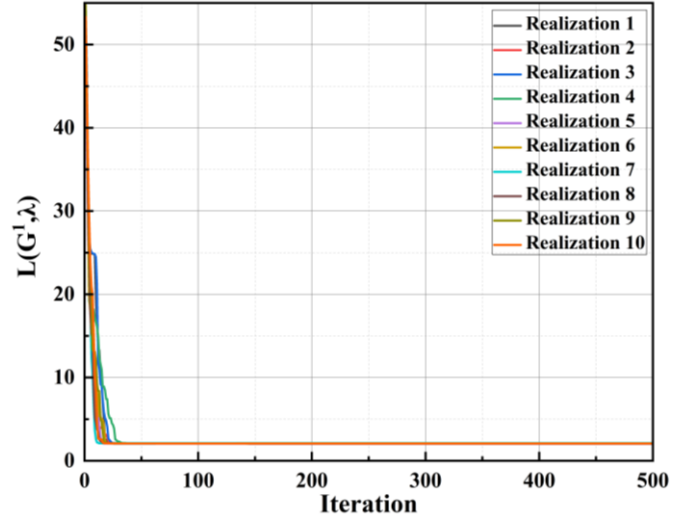


**Fig. 4.** Converging curves of the WOA algorithm

Compared with PSO [13], WOA can jump out of the local optimal solution because it can more effectively balance global exploration and local development during the optimization process. After recording the transmission matrix  $[A^1 A^2]$ , the WOA algorithm is applied to find the pre-compensation matrix  $G^1$  that satisfies the objective function in Eq. (4). As mentioned above, ten realizations are run to find the global optimal solution. The convergence curves of the WOA algorithm are shown in Fig. 4. It can be seen that all ten realizations converge to the global optimal solution, indicating that the possibility of finding the global optimal solution using the proposed WOA algorithm is very high. Based on the results of the ten realizations, the pre-compensation matrix  $G^1$  with the function  $L(G^1, \lambda)$  is selected as the estimated value of the transfer matrix  $[A^1 A^2]$ .

## IV. EXPERIMENT AND VALIDATION

### A. Experimental system

As shown in Fig. 5, the experimental system consists of a two-port Vector Network Analyzer (VNA), CE, probe antennas, DUT antennas, switches and power divider. The antenna arrangement in the anechoic chamber is illustrated in Fig. 6. The VNA is configured with 801 frequency samples, scanning frequencies from 3.56 GHz to 3.64 GHz, with an intermediate frequency bandwidth of 1 kHz and a transmission power of -5dBm. As shown in Fig. 5, the four probe antennas are arranged on the same board, while the DUT antennas for different DUTs are arranged on two separate boards.

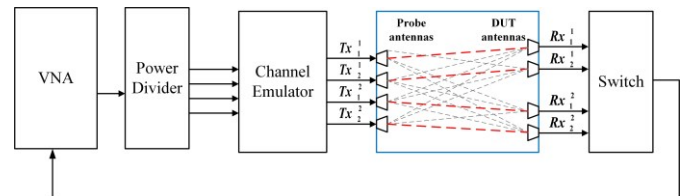


**Fig. 5.** The diagram of the experiment.



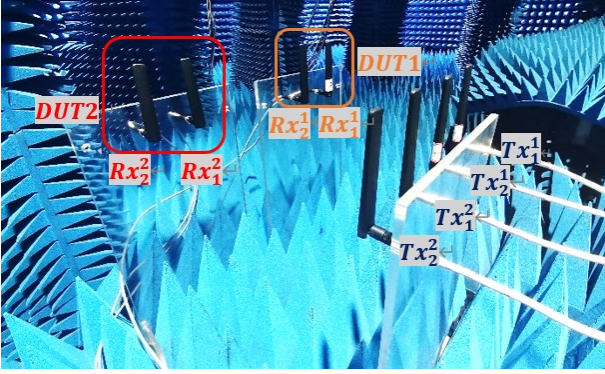


Fig. 6. The experiment in an anechoic chamber.

### B. Calibration

As described in [14], the transmission matrices  $A^1$  and  $A^2$  are estimated during the calibration process. Both the input and output ports of the CE are equipped with phase shifters and attenuators, which are all set to  $0^\circ$  and 0 dB, respectively. The complex coefficients in the transmission matrix from the probe antennas to the DUT antennas can be expressed as  $\hat{a}_{ik}^n = \alpha_{ik}^n e^{j\varphi_{ik}^n}$ , where  $\alpha_{ik}^n$  represents the amplitude term of the transmission coefficient from the  $k$ th probe antenna to the  $i$ th DUT antenna of the  $n$ th DUT, and  $\varphi_{ik}^n$  represents the corresponding phase term,  $k \in [1, 4]$ ,  $i \in [1, 2]$ ,  $n \in [1, 2]$ . The  $k$ th probe antenna is turned on while the remaining three probe antennas are turned off. The amplitude and phase of the signal received by each DUT antenna are recorded respectively, denoted as  $\alpha_{ik}^n$ . The remaining three probe antennas repeat this switching operation to obtain the transmission matrices  $A^1$  and  $A^2$ . Note that if the condition number of the transmission matrix  $A^n$  is too large, the matrix is too ill-conditioned to make the inversion process difficult, resulting in poor isolation.

### C. Measurement Result

In order to intuitively illustrate the isolation between different DUTs and the wireless connection of a single DUT, a simple diagonal direct channel is adopted for the experiment. For simplicity, the channel to each DUT's probe antenna has two rays. Fig. 7 and Fig. 8 show the comparison between the target signal and the actual received signal in the frequency domain and time domain for the four Rx antennas of two DUTs, respectively. It can be seen from Fig. 7 that the trend of the received signal and the target signal of each connection is consistent, but the signal has a slight fluctuation. This is because each connection cannot completely isolate the interference from other transmitted signals. In Fig. 8, the rays on each DUT's receiving antenna are consistent with the ideal rays, and the power of unexpected rays are less than -15dB. The experimental results show that two channels with different power delay profile (PDP) are successfully reconstructed with interference rejection if more than 15dB.

## V. CONCLUSION

In practice, the spatial distribution of different users has a significant impact on BS performance. This distribution affects signal reception quality and may lead to more complex interference issues when the BS processes signals from multiple users. Therefore, multi-user OTA testing

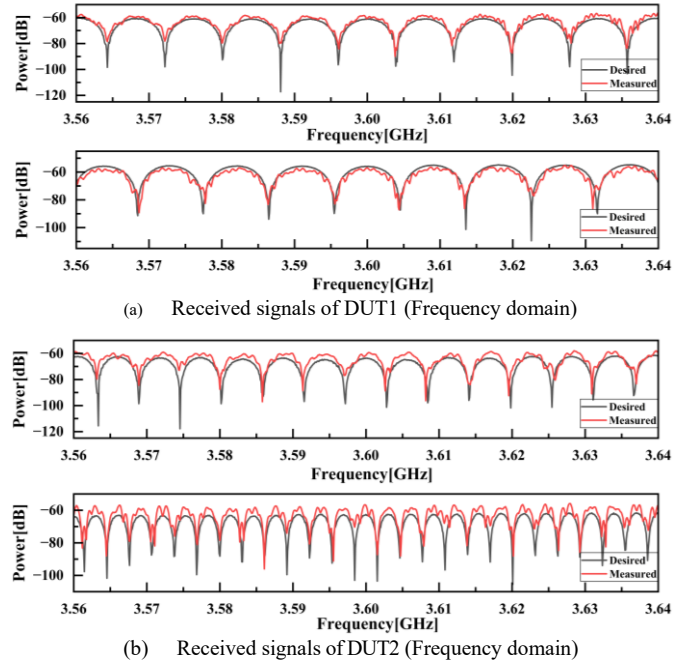


Fig. 7. The measured and desired signals in frequency domain.

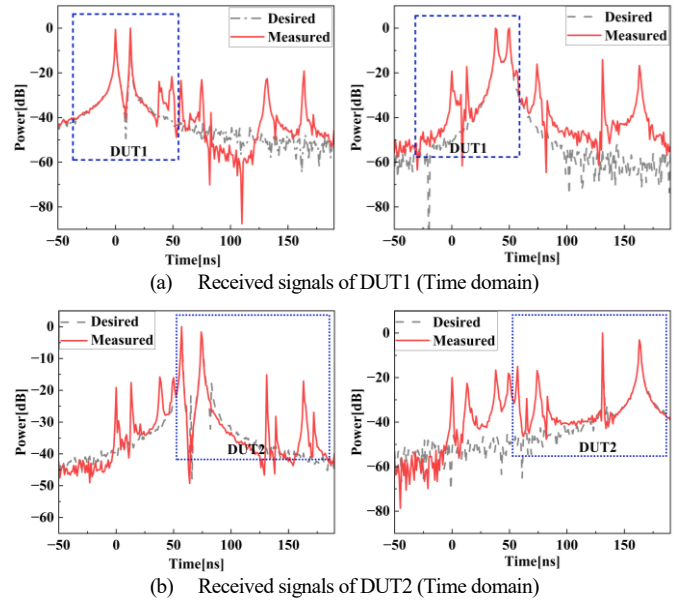


Fig. 8. The measured and desired signals in time domain.

is essential to evaluate the performance of wireless communication systems in real environments. In this paper, a multi-user OTA performance testing method is first proposed, and a VNA-based experiment for a two  $2 \times 2$  MIMO channel reconstruction is conducted. The transmission matrix is estimated based on the signal received by the DUT antennas, and the pre-compensation matrix of the multi-user wireless cable is determined according to the WOA algorithm. The test results show that the system can support multi-user OTA test, with an isolation greater than 15dB.

## REFERENCES

- [1] E. G. Larsson, O. Edfors, F. Tufvesson and T. L. Marzetta, "Massive mimo for next generation wireless systems," *IEEE Commun. Mag.*, vol. 52, no. 2, pp. 186-195, Feb. 2014.
- [2] R. W. Heath, *et al.*, "An overview of signal processing techniques for millimeter wave mimos systems," *IEEE J. Sel. Top. Signal Process.*, vol. 10, no. 3, pp. 436-453, Apr. 2016.
- [3] S. Zhe *et al.*, "Probe selection and power weighting for mimo ota testing with multiple users," in *19th International Conference on Communication Technology (ICCT)*, 2019, pp. 810-813.
- [4] F. Rusek *et al.*, "Scaling up mimo: opportunities and challenges with very large arrays," *IEEE Signal Process Mag.*, vol. 30, no. 1, pp. 40-60, Jan. 2013.
- [5] Kyösti *et al.*, "Channel modelling for multiprobe over-the-air MIMO testing," *Int. J. Antennas Propag.*, vol. 62, no 4, pp. 2130-2139, 2014.
- [6] X. Chen, "Throughput modeling and measurement in an isotropic-scattering reverberation chamber," *IEEE Trans. Antennas Propag.*, vol. 62, no. 4, pp. 2130-2139, Apr. 2014.
- [7] *Study on Radiated Metrics and Test Methodology for the Verification of Multi-Antenna Reception Performance of NR User Equipment (UE)*, document 3GPP TR 38.827 V16.8.0, 2022.
- [8] P. -S. Kildal *et al.*, "Characterization of reverberation chambers for ota measurements of wireless devices: physical formulations of channel matrix and new uncertainty formula," *IEEE Trans. Antennas Propag.*, vol. 60, no. 8, pp. 3875-3891, Aug. 2012.
- [9] P. Kyösti, T. Jaemsae, and J. P. Nuutinen, "Channel modelling for multiprobe over-the-air mimo testing," *International Journal of Antennas and Propagation.*, vol. 2012, no. PT.3, pp. 22.1–22.11, 2012.
- [10] W. Fan *et al.*, "MIMO terminal performance evaluation with a novel wireless cable method," *IEEE Trans. Antennas Propag.*, vol. 65, no. 9, pp. 4803-4814, Sept. 2017.
- [11] W. Fan *et al.*, "Wireless Cable Testing for MIMO Radios: A Compact and Cost-Effective 5G Radio Performance Test Solution," *IEEE Trans. Antennas Propag.*, vol. 71, no. 10, pp. 8239-8249, Oct. 2023.
- [12] Seyedali Mirjalili, Andrew Lewis, "The whale optimization algorithm," *Adv. Eng. Software.*, vol 95, pp. 51-67, 2016.
- [13] F. Zhang *et al.*, "Performance testing of mimo device with the wireless cable method based on particle swarm optimization algorithm," in *International Workshop on Antenna Technology (iWAT)*, 2018, pp. 1-4.
- [14] F. Zhang, W. Fan and Z. Wang, "Achieving wireless cable testing of high-order mimo devices with a novel closed-form calibration method," *IEEE Trans. Antennas Propag.*, vol. 69, no. 1, pp. 478-487, Jan. 2021.